# *Strategically designed antifibrotic gold nanoparticles to prevent collagen fibril formation*

Collagen is an important structural protein that provides crucial mechanical framework which is vital to many structural and functional roles of tissues of its existence including the extra cellular matrix (ECM) (B Brodsky & Ramshaw, 1997). In tissues, triple helical (Ramachandran & Kartha, 1954) collagen molecules undergo a process of self-assembly to form supramolecular structures such as D-periodic fibrils of type I collagen, networks of type-IV collagen (Yurchenco & Ruben, 1988) and arrays of type VIII collagen (Stephan, Sherratt, Hodson, Shuttleworth, & Kielty, 2004). Though self-assembly process of collagen triple-helical molecules is considered as a fundamental process in biology, unregulated collagen fibril formation has been implicated in many medical complications such as thrombosis, restenosis and tissue stiffness related heart diseases. Exposed collagen is known to trigger thrombosis which is directly linked to myocardial infarction and stroke (Farndale, Sixma, Barnes, & De Groot, 2004). Abnormalities linked to type VIII collagen is known to induce atherosclerosis lesions and plaque formation (Plenz, Deng, Robenek, & Völker, 2003) and rupture of such plaques causes cardiac arrest as well as stroke. Uncontrolled accumulation of collagen at the sites where stents are deployed after angioplasty is also known to cause blockage of cardiac arteries (Lafont et al., 1999.; Osherov, et al.,2011.). Collagen is also linked to tissue fibrosis severities (Burke et al., 2007; Steplewski & Fertala, 2012) including hypertensive heart diseases (Cecelja & Chowienczyk, 2012). Since accumulation of unregulated collagen is linked to many diseases, it is essential to find potential inhibitors against collagen fibril formation. Such a strategy to target collagen fibril formation may perhaps be useful in treating collagen linked diseases(Steplewski & Fertala, 2012). Targeting the driving forces that are known to promote the onset of collagen fibril formation may possibly become an effective strategy for inhibition of collagen self-assembly (Steplewski & Fertala, 2012)(Persikov, Ramshaw, & Brodsky, 2005). Aromatic-proline interactions(Kar et al., 2009a; Persikov et al., 2005) and hydrophobic interactions (Cejas et al., 2008) are considered as the critical factors for promoting self-assembly of triple helical molecules into higher order structures.

Here in this chapter stable gold nanoparticles surface-functionalized with selected aromatic/hydrophobic residues have been synthesized and effect of these nanoparticles on fibril formation of type I collagen has been studied using a combination of both biophysical and computational methods.

## 6.1 EFFECT OF GOLD NANOPARTICLES COATED WITH AROMATIC RESIDUES ON COLLAGEN FIBRIL FORMATION.

This chapter hypothesize that, specifically targeting the hydroxyproline mediated interactions between collagen molecules will possibly prevent the process of collagen fibril formation. Based on this hypothesis, in this work, gold nanoparticles surface-functionalized with hydroxyproline (AuNPs[HYP]) were synthesized. Surface functionalized gold nanoparticles have recently shown to interfere with the self-assembly processes of amyloidogenic proteins that is believed to be mainly driven by hydrophobic interactions (Anand, Dubey, Shekhawat, & Kar, 2016; Dubey et al., 2015). Successful synthesis of amino acid coated gold nanoparticles has been reported where the gold nanoparticles are functionalized with amino acids through their amino group, allowing the carbonyl and the side chain groups of the conjugated-amino acid to interact with the binding site residues of the protein.(Anand et al., 2016; Dubey et al., 2015; Selvakannan et al., 2013). Some studies have also proposed that inhibition efficacies of some compounds are greatly enhanced when the inhibitor molecules are surface

functionalized(Anand et al., 2016; Dubey et al., 2015) . The inhibition effect of AuNPs**HYP** nanoparticles on the fibril formation of type-I collagen (both from rat tail tendon and calf skin sources) under *in vitro* conditions, maintaining physiological pH at 7.4 (PBS) and temperature at 37°C was studied. Type I collagen is the most abundant in human body. *In vitro* fibril formation of type I collagen has been studied by several researchers including the report by (Williams et al., 1978) Hence, type I collagen was chosen as a model convenient system for studying the process of collagen fibril formation and its inhibition in the presence *Hyp* coated gold nanoparticles. In addition to AuNPs**HYP**, gold nanoparticles coated with proline (AuNPs**PRO**), tryptophan (AuNPs**TRP**) and glycine (AuNPs**GLY**) were also examined for comparative studies. Studies have also been conducted to analyze the binding affinity of AuNPs**HYP** with a collagen model peptide, (Pro-Hyp-Gly)$_{10}$, using isothermal titration calorimetry (ITC). Further, molecular interaction between collagen triple helical model peptides and hydroxyproline molecule has been studied using computational docking tools. Finally, the hemocompatibility of these amino acid coated nanoparticles was also accessed.

### 6.1.1 Synthesis and characterization of gold nanoparticles.

Gold nanoparticles coated with phenylalanine (AuNPs**PHE**), tryptophan (AuNPs**TRP**) proline (AuNPs**PRO**) and hydroxyproline (AuNPs**HYP**) were synthesized by following the established protocol see methods section annexure A. The UV-Visible spectra of these nanoparticles showed its respective SPR peak for gold nanoparticles around ~530 nm (Figures 6.1, 6.2, 6.3 and 6.4 panel e). Dynamic light scattering data of AuNPs samples clearly showed a homogeneous population of nanoparticles with average hydrodynamic radius of ~10 to 50 nm (Figures 6.1, 6.2, 6.3 and 6.4 panel g). The surface charge values obtained from Zeta potential measurements for AuNPs TRP, AuNPs PRO, AuNPs GLY, AuNPs HYP and AuNPs PHE were found to be -28.46 mV, -45.5mV, -72.6mV and -54.9mV respectively as shown in the figures 6.1, 6.2, 6.3 and 6.4 panel h. Transmission electron microscopy (TEM) images further confirmed the formation of spherical homogenous species of AuNPs TRP, AuNPs PRO, AuNPs GLY AuNPs PHE and AuNPs HYP (Figures 6.1, 6.2, 6.3 and 6.5 panel b). To elucidate the chemistry of surface functionalization of amino acid molecules with the nanoparticles, ATR-FTIR measurements were conducted for these functionalized nanoparticles. Panel e of figures 6.1, 6.2, 6.3, 6.4 and 6.5 displays the FTIR signatures obtained for surface-functionalized gold nanoparticles.
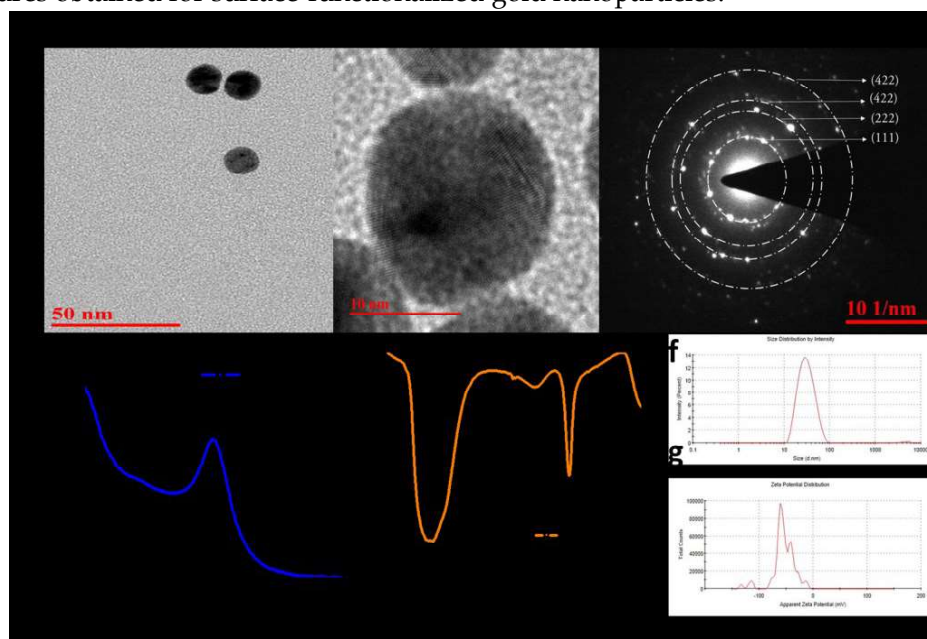


**Figure 6.1. Characterization of Phenylalanine coated gold nanoparticles (AuNPs**PHE**) (a)**TEM **(b)** HRTEM images displaying the evenly sized (~20nm) spherical AuNPs**PHE** **(b)** The selected area electron diffraction pattern (SAED) of AuNPs**PHE**. The Scherrer rings indicate the FCC gold which is nanocrystalline in nature. **(d)** UV-Vis

spectrum of AuNPs[PHE](e) FTIR Spectra of AuNPs[PHE] (f) Dynamic Light Scattering (DLS) peak of AuNPs[PHE] (g) Zeta potential peak of AuNPs[PHE].
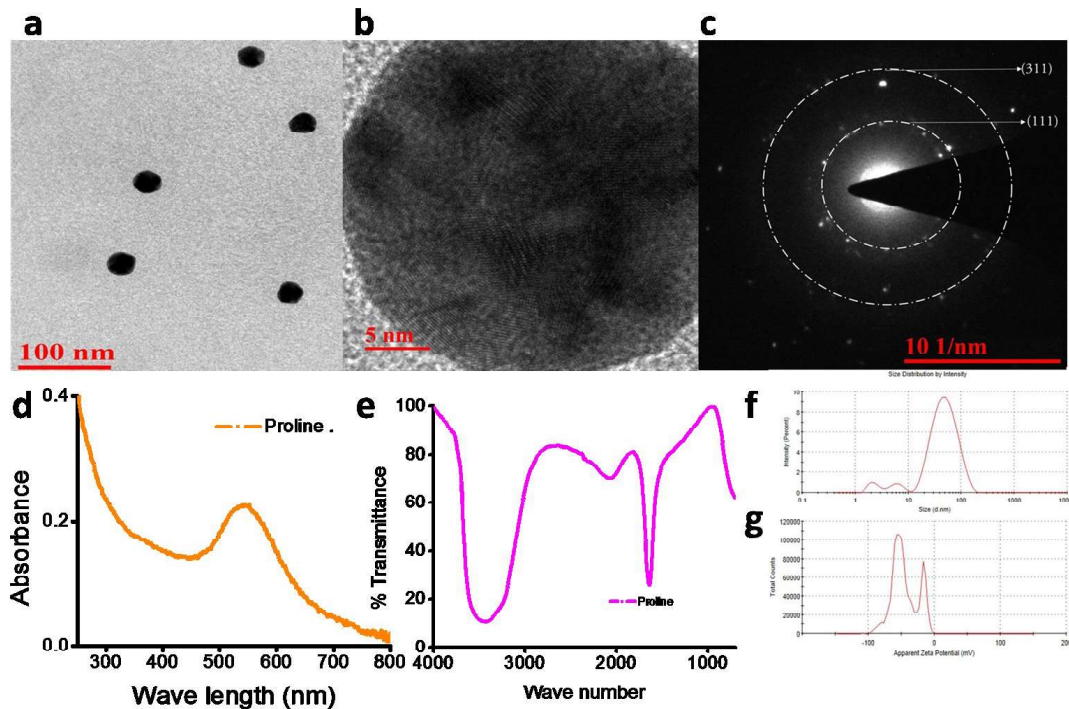


**Figure 6.2. Characterization Proline coated gold nanoparticles (AuNPs[PRO]) (a)**TEM and HRTEM images displaying the evenly sized (~20nm) spherical AuNPs[PRO] **(b)** The selected area electron diffraction pattern (SAED) of AuNPs[PRO]. The Scherrer rings indicate the FCC gold which is nanocrystalline in nature. **(d)** UV-Vis spectrum of AuNPs[PRO]**(e)** FTIR Spectra of AuNPs[PRO] **(f)** Dynamic Light Scattering (DLS) peak of AuNPs[PRO] **(g)** Zeta potential peak of AuNPs[PRO].
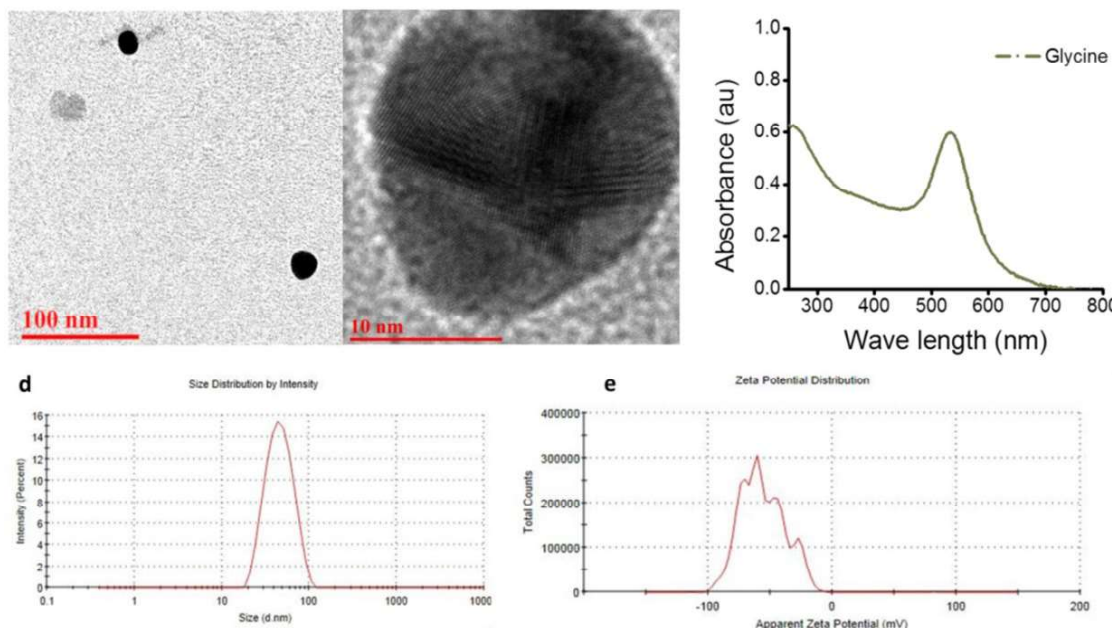


**Figure 6.3Characterization glycine coated gold nanoparticles (AuNPs[GLY]) (a)**TEM displaying the evenly sized (~20nm) spherical AuNPs[GLY]**(b)**HRTEM images of the AuNPs[GLY]**(c)**UV-Vis spectrum of AuNPs[GLY]**(d)** Dynamic Light Scattering (DLS) peak of AuNPs[GLY]**(e)**Zeta potential peak of AuNPs[GLY]
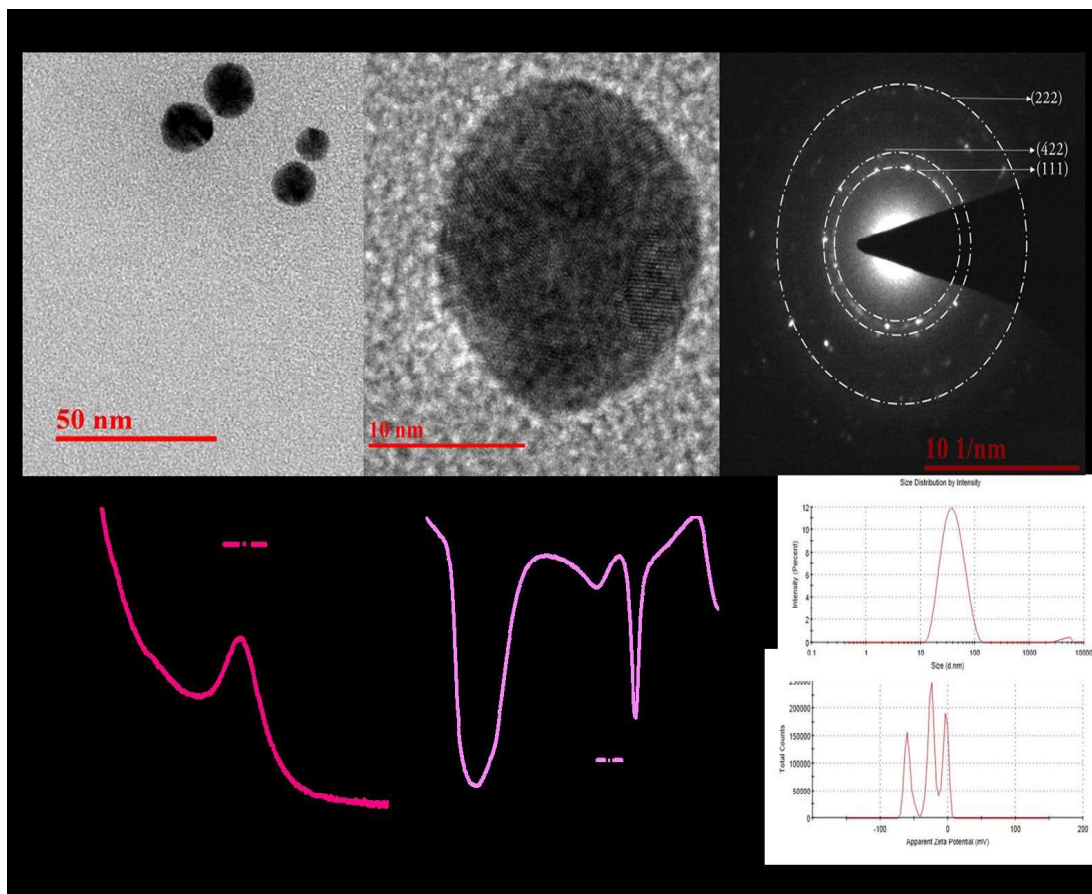
**Figure 6.4 Characterization Tryptophan coated gold nanoparticles (AuNPs^TRP) (a)**TEM and HRTEM images displaying the evenly sized (~20nm) spherical AuNPs^TRP **(b)** The selected area electron diffraction pattern (SAED) of AuNPs^TRP. The Scherrer rings indicate the FCC gold which is nanocrystalline in nature. **(d)** UV-Vis spectrum of AuNPs^TRP**(e)** FTIR Spectra of AuNPs^TRP**(f)** Dynamic Light Scattering (DLS) peak of AuNPs^TRP **(g)** Zeta potential peak of AuNPs^TRP.

The spectra revealed that the carbonyl groups are exposed outside due to the presence of its carbonyl stretching frequency around 1740cm$^{-1}$ for AuNPs^GLY, AuNPs^PRO, AuNPs^PHE and AuNPs^TRP (Dubey et al. 2015c) (Selvakannan et al. 2013)(Daima et al. 2011)(H.K. Daima, PR. Selvakannan, S.K. Bhargava, S.K. Shastry 2014). To further characterize the intrinsic structural properties of the AuNPs^HYP, AuNPs^PRO, AuNPs ^GLY, AuNPs^PHE and AuNPs^TRP nanoparticles, high-resolution TEM (HRTEM) was performed which confirmed the polycrystalline nature of the nanoparticles (Figures 6.1, 6.2, 6.3, 6.4and 6.5 panel c). To throw light into the nature of alignment of crystalline fringes, HRTEM was done and the results revealed the polycrystalline nature of these functionalized nanoparticles. It was important to examined SAED (the selected area electron diffraction ) pattern of these AuNPs^HYP, AuNPs^PRO, AuNPs^PHE and AuNPs^TRP nanoparticles  using image J software and the ring patterns of the obtained data revealed the presence of  (220), (200) and (111)  for AuNPs^HYP, (111) and (311) for AuNPs^PRO (222), (422) and (111) for  AuNPs^TRP (220), (311), and (420)  and (422), (222) and (111) indexed face-centered cubic crystal (FCC) structure for all the gold nanoparticles (Figures 6.1, 6.2, 6.3, 6.4 and 6.5 panel c). All these synthesized gold nanoparticles were found to be highly stable for more than nine months.
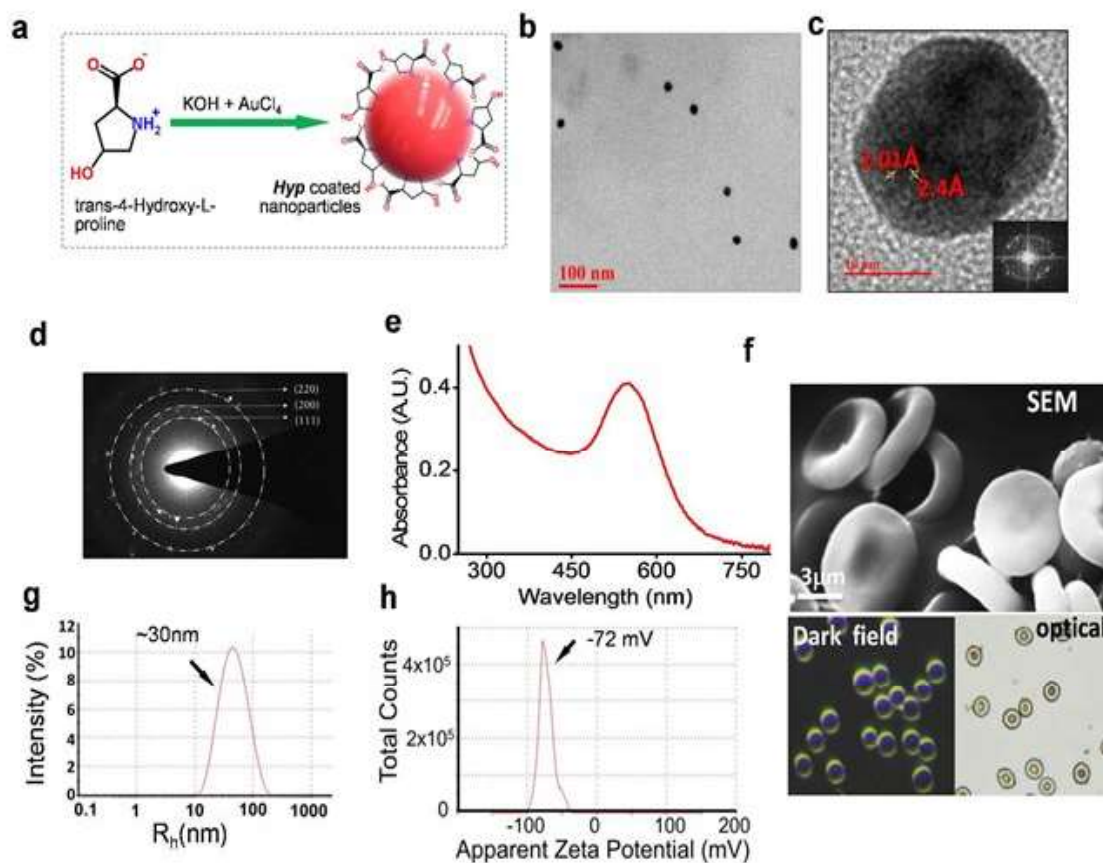
**Figure 6.5 Biophysical characterization of hydroxyproline coated gold nanoparticles (AuNPs$^{HYP}$).**
(a) Schematic representation of the surface functionalized gold nanoparticles. (b) TEM images displaying the evenly sized (~30nm) spherical AuNPs$^{HYP}$ (c) HR TEM data showing a fringe spacing of 2.01 Å and 2.4Å. Inset shows splitting of spots in the FFT image. (d)A selected area electron diffraction pattern (SAED) of AuNPsHYP. The Scherrer ring patterns indicate the nanocrystalline nature of FCC gold. (e) UV-Vis spectrum of AuNPs$^{HYP}$ with an absorption maximum around ~530 nm due to surface plasma resonance. (f)SEM (scale bar 3μM), optical and dark field microscopy images of intact RBC sample in the presence of AuNPs$^{HYP}$. (g) Dynamic Light Scattering (DLS) data of AuNPs$^{HYP}$, showing an average diameter of ~20-30 nm. (h) Zeta potential measurements of AuNPs$^{HYP}$ sample.

## 6.1.2 Biocompatibility studies of synthesized gold nanoparticles.

To understand the implication of the hydroxyproline coated gold nanoparticles in biomedical applications, the hemocompatibility of these nanoparticle-based inhibitors on human RBCs were examined. The toxicity effect of these nanoparticles on the intact red blood cells were tested by following the established protocol for hemolysis assay (Mattson et al. 1997). Data generated from the hemolysis assay experiments showed no indication of lysis in the presence of AuNPs$^{HYP}$ (Figure 6.5f). Hemocompatibility of these nanoparticles based inhibitors were confirmed by scanning electron microscopy (SEM), optical and dark field microscopy as shown in Figure 6.5f

## 6.1.3 Effect of surface functionalized gold nanoparticles on collagen fibril formation.

Collagen fibril formation was initiated by incubating the acid-soluble type I collagen solution in PBS buffer (pH 7.4) at 37°C and the optical density of the sample at 313 nm was monitored as a function of time to record the onset of collagen self-assembly. The turbidity curve obtained for control collagen sample showed a typical pattern(Dubey & Kar, 2014; Perumal et al., 2015) consisting of a negligible lag phase, a growth phase and a plateau phase (▬▬ curve Figure 6.6a).
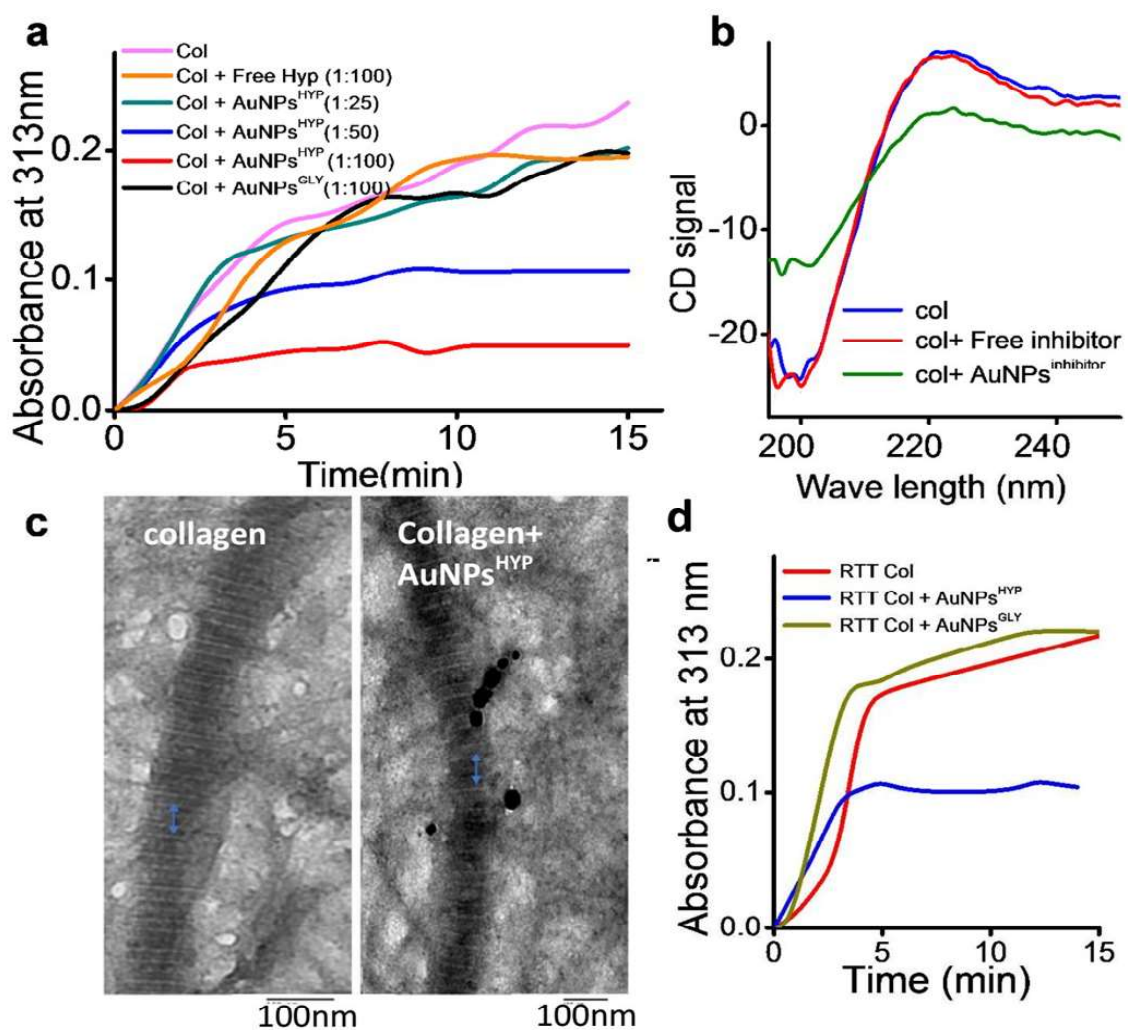
**Figure 6.6: Inhibition effect of AuNPs^HYP on fibril formation process of type I collagen:** (a) Turbidity data showing fibril formation of calf skin collagen (0.3 mg.ml-1) in the presence and in the absence of inhibitors under physiological temperature 37°C and in PBS buffer. Molar ratio of collagen: inhibitor is given in the parentheses: (━━) control collagen; (━━) collagen + Hyp (at 1:100); (━━) collagen + AuNPs^HYP (at 1:25); (━━) collagen + AuNPs^HYP (at 1:50); (━━) collagen + AuNPs^HYP (at 1:100); (━━) collagen + AuNPs^GLY (at 1:100); **(b)** CD profiles collagen after fibril formation. (━━) control collagen; (━━) collagen + free Hyp (1:100 molar ratio); (━━) collagen + AuNPs^HYP (1:100 molar ratio). All CD spectra shown here were base line subtracted. **(c)** TEM images showing the fibril morphology of collagen fibrils in the presence and in the absence of inhibitor. Scale bar 100nm. **(d)** Inhibition of fibril formation of type I collagen from rat tail tendon: (━━) control collagen; (━━) collagen + AuNPs^HYP (at 1:100); (━━) collagen + AuNPs^GLY (at 1:100). All turbidity curves shown in this figure are the average representative of three acquisitions.

However, in the presence of AuNPs^HYP, gradual suppression of such fibril formation was observed in a dose dependent manner (Figure 6.6a). Though the lag time was not observed to be significantly affected by the presence of these inhibitors, the extent of the fibril formation was substantially reduced. Such inhibition effect, without any delay in the lag phase was recently observed in a study on inhibition of collagen fibril formation(Perumal et al., 2015). No such inhibition effect on collagen fibril formation was observed in the presence of free hydroxyproline (Figure 6.6a, ━━ curve) and control gold nanoparticles surface functionalized with glycine (AuNPs^GLY) at similar concentrations (Figure 6.6a, ━━ curve).
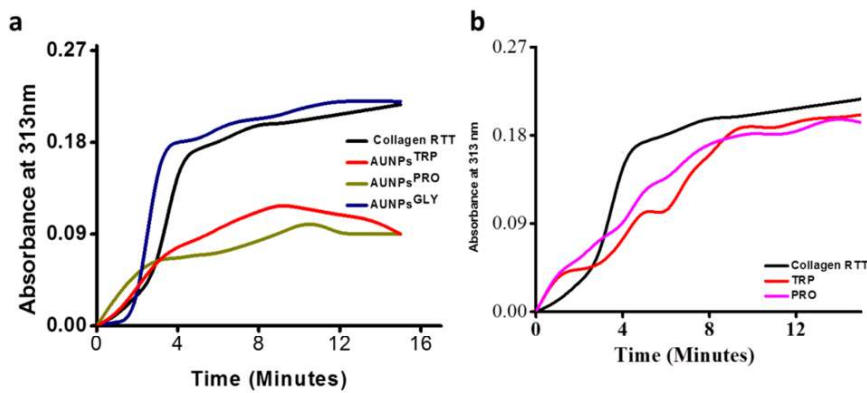
**Figure 6.7: Effect of proline, tryptophan and glycine coated nanoparti5cles on fibril formation process of type 1 collagen.** Turbidity data showing fibril formation of calf skin collagen in the presence and in the absence Of inhibitors under physiological temperature 37°C and in PBS at pH 7: (▬▬) control collagen; (▬▬) collagen + AuNPs $^{TRP}$ at 1:100 molar ratio; (▬▬) collagen + AuNPs $^{PRO}$ at 1:100 molar ratio; (▬▬) collagen + AuNPs $^{GLY}$ at 1:100 molar ratio. **(b)**Effect of free uncoated amino acids on collagen fibril formation; (▬▬) control collagen; (▬▬) collagen+ free Trp at 1:100 molar ratio; (▬▬) collagen+ free Pro 1:100 molar ratio. All turbidity curves shown in this figure are the average representative of three acquisitions.

The characteristic properties of the AuNPs$^{GLY}$ sample have been given in the (Figure 6.3). This result suggests the significance of surface-functionalized hydroxyproline residues to interfere with the collagen fibril formation. Conformational changes occur in the collagen molecule during their assembly into fibrils (George A et al. 1991) and under fibril forming condition, the triple helical structure of the semi-flexible collagen molecule is believed to be perfected during lag phase, facilitating nucleation and intramolecular interaction (Kadler et al. 1996). It is possible that the presence of AuNPs$^{HYP}$ at higher concentration (1:100) can interfere with both the nucleation phase and the growth phase of the fibril formation process of type I collagen. It is also interesting to see that similar slight-delay in the lag phase was observed in the presence control gold nanoparticles (AuNPs$^{GLY}$ at 1:100), however, the fibril formation process was not suppressed in the presence of AuNPs$^{GLY}$ (Figure 6.6a, ▬▬ curve). It is possible that AuNPs$^{GLY}$ (at 1:100) can influence the nucleation event to some extent which may not be sufficient to block the intermolecular interactions leading to collagen-fibril assembly.

To generalize this inhibition effect on type I collagen, the effect of AuNPs$^{HYP}$ on fibril formation of type I collagen obtained from rat tail tendon (RTT) was examined (Annexure). The turbidity data as shown Figure 6.7 clearly shows similar inhibition effect as was seen for calf-skin collagen sample (Figure 6.6a).
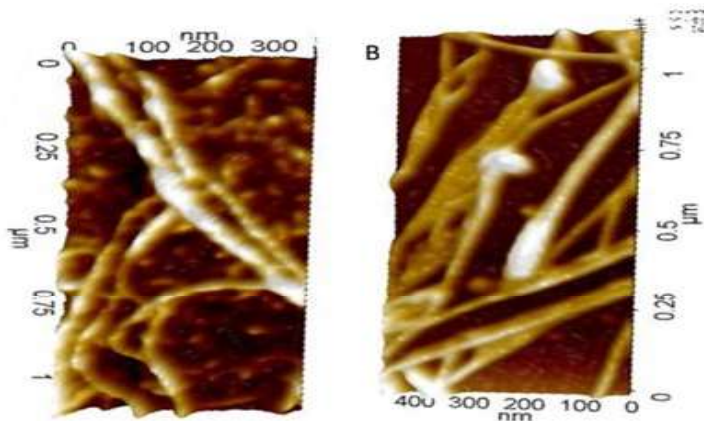


**Figure 6.8: Atomic Force microscopic image of mature fibrils.** AFM images of the collagen fibrils obtained from both inhibited (A)and control(B)reactions

The morphology of the samples of collagen fibrils formed both in the absence and in the presence of AuNPs[HYP] inhibitors was observed. Characteristic features of fibrils, obtained from both the sources remained unchanged (Figure 6.6c). The atomic force microscopy (AFM) images also showed similar fibril morphology for collagen samples obtained from inhibited and uninhibited reactions (Figure 6.8). The CD signal of the fibril samples and the CD profiles showed a typical positive peak at ~222 nm for all the samples, confirming the presence of triple helical conformation in the fibrils (Figure 6.6b). However, the intensity of the triple-helix peak at 222 nm for collagen fibrils obtained from the inhibited reaction was observed to be lower than the peaks obtained for control collagen fibrils. Such difference in the signal intensity maybe attributed to the lower fibril concentration in an inhibited reaction. Both CD and AFM data suggest that the inhibition effect mediated by AuNPs[HYP] may be achieved without altering the normal collagen fibril formation pathway.

### 6.1.4 Computational Docking Studies of amino acids with Selected Triple-Helical Collagen Model Peptides

To further understand the molecular interaction between hydroxyproline and triple helical domains of collagen, molecular docking studies were performed using selected triple helical collagen model peptides (figure 6.10c). Using AutoDock Vina wizard, blind docking studies were carried out and the obtained data are shown in Figure 6.10 a,b. The structures of the triple helix-hydroxyproline docked complexes predict formation of strong H-bonding interactions mediated by C=O and hydroxyl groups of the *Hyp* (Figure 6.10). The value of binding affinity energy obtained for peptide-Hyp interactions was found to be -12.9 kJ.mol$^{-1}$ for 1CAG peptide and was observed to be -13.5 kJ.mol$^{-1}$ for 1Q7D peptide.
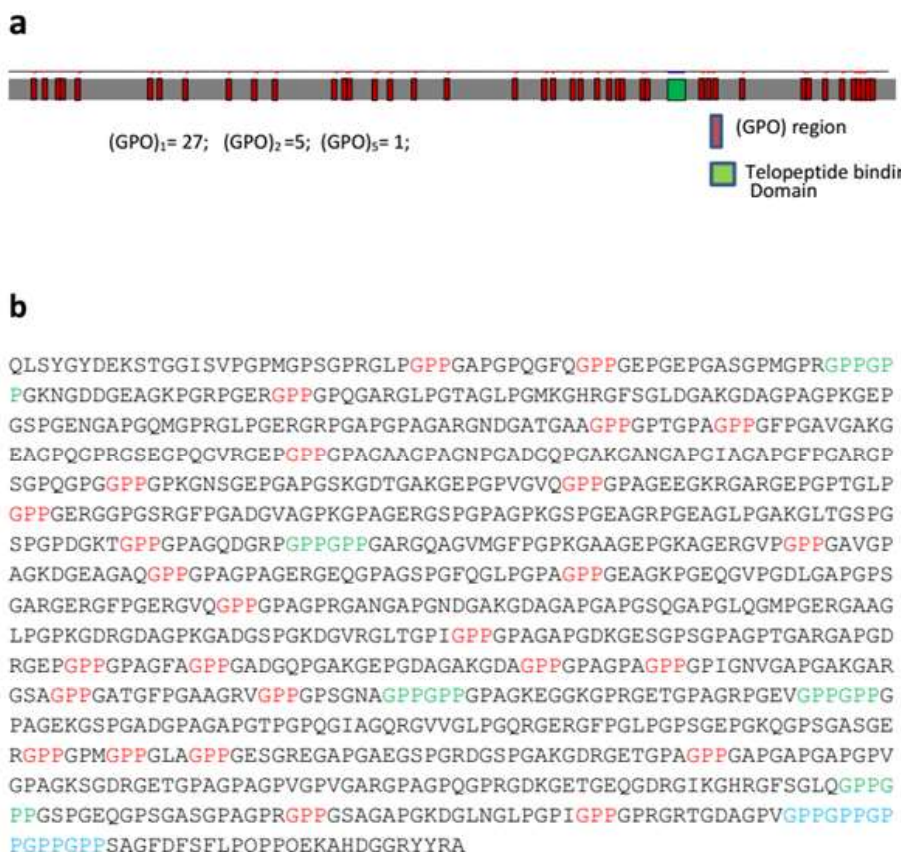


**Figure 6.9: Analysis of collagen sequence for GPO stretches. (a)** A proportionate graphical representation of α1 collagen (type I) sequence displaying the frequent occurrence of GPO sequences (red) throughout the triple helical region of the peptide. The green area shows the telopeptide binding region within the collagen sequence. **(b).** Sequence of α1 chain of type I collagen.

The IQ7D peptide has the sequence GFOFER, that is derived from the triple helical telopeptide binding region (T-TBR) of α-1 chain of the type I collagen (Chung, Steplewski, Chung, Uitto, & Fertala, 2008). Such sequence stretch with GFOGER span is also known to occur in the integrin binding region of the collagen sequence(Emsley, Knight, Farndale, & Barnes, 2004). It is well known that the telopeptide binding region (T-TBR), ([776]GIAGQRGVVGLOGQRGFOGERG[796]) (figure 6.9) is known to play a key role in initiating the fibril formation of type I collagen. This is achieved specifically by interacting with the non-helical telopeptide sequence residues of the interacting collagen molecule(Chung et al., 2008; Steplewski & Fertala, 2012). Notably, as evident from the docking data (Figure 6.10 and 6.11), viable contacts with the *Arg, Gly and Hyp* (belonging to the same chain) of the triple-helical GFOGER domain were observed. Such data suggest binding of *Hyp* to the T-TBR region of type I collagen could be one of the factors necessary for the inhibition effect.
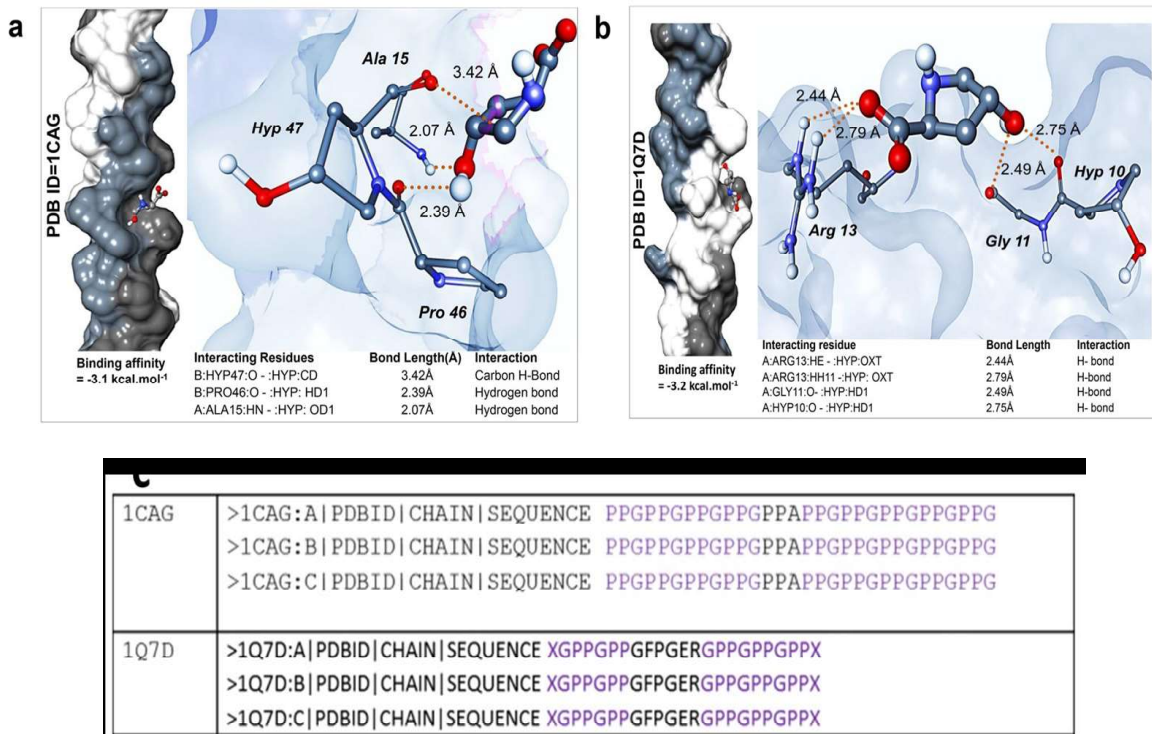


**Figure 6.10 Interaction of hydroxyproline with the triple-helical collagen model peptides.** (a)Docking studies of the collagen model peptide (POGPOGPOGPOGPOAPOGPOGPOGPOGPOG) (PDB-ID-1CAG) showing three viable H-bonding interactions as labelled. Binding affinity for this interaction was -3.1 kcal.mol-1. (b) Molecular docking studies of the collagen model peptide (PDB ID 1Q7D) (XGPOGPOGFOGERGPOGPOGPOX) showing four strong hydrogen bond interactions as labelled. Binding affinity for this interaction was -3.2 kcal.mol-1. (c) Sequence of the peptides.

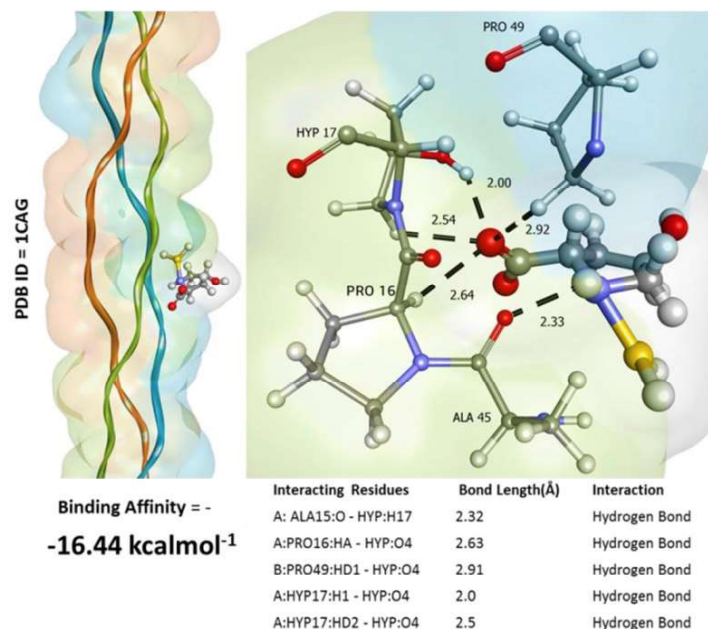| Interacting Residues | Bond Length(Å) | Interaction |
|---|---|---|
| A: ALA15:O - HYP:H17 | 2.32 | Hydrogen Bond |
| A:PRO16:HA - HYP:O4 | 2.63 | Hydrogen Bond |
| B:PRO49:HD1 - HYP:O4 | 2.91 | Hydrogen Bond |
| A:HYP17:H1 - HYP:O4 | 2.0 | Hydrogen Bond |
| A:HYP17:HD2 - HYP:O4 | 2.5 | Hydrogen Bond |

**Figure 6.11 Summary of the modified Hyp AU –Collagen(1CAG) interaction.** Interaction of the modified Hyp (in which a gold atom is attached to the –NH moiety) with collagen model peptide 1CAG.

## 6.1.5 Interaction of triple-helical collagen peptide with AuNPsHYP by Isothermal Titration Calorimetry (ITC).

Since type I collagen triple-helical molecules in PBS tend to aggregate, it was difficult to directly perform ITC experiments on RTT type I collagen. Hence, for these studies a well-studied collagen model peptide (Pro-Hyp-Gly)$_{10}$ (Kar et al., 2008) which attains a very stable triple helical conformation in PBS buffer was procured . Before ITC measurements, the peptide was dissolved in PBS buffer and kept at low temperature at least for three days to allow the formation of triple-helical structures. The triple-helical conformation of the (Pro-Hyp-Gly)$_{10}$ peptide was examined by monitoring the CD signal that displayed a positive peak at 222 nm (Figure 6.12).
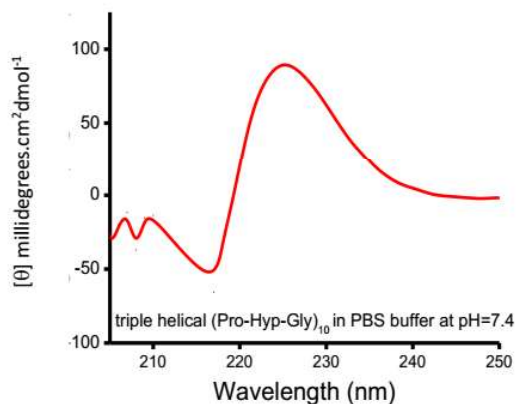


**Figure 6.12:** Circular Dichroism signal of the collagen model peptide (Pro-Hyp-Gly)10 in PBS buffer at pH 7 (concentration = 1 mg.ml$^{-1}$). The data confirmed the formation of triple-helical molecules of the peptide POG10. This sample was used for binding studies with AuNPs$^{HYP}$ nanoparticles.
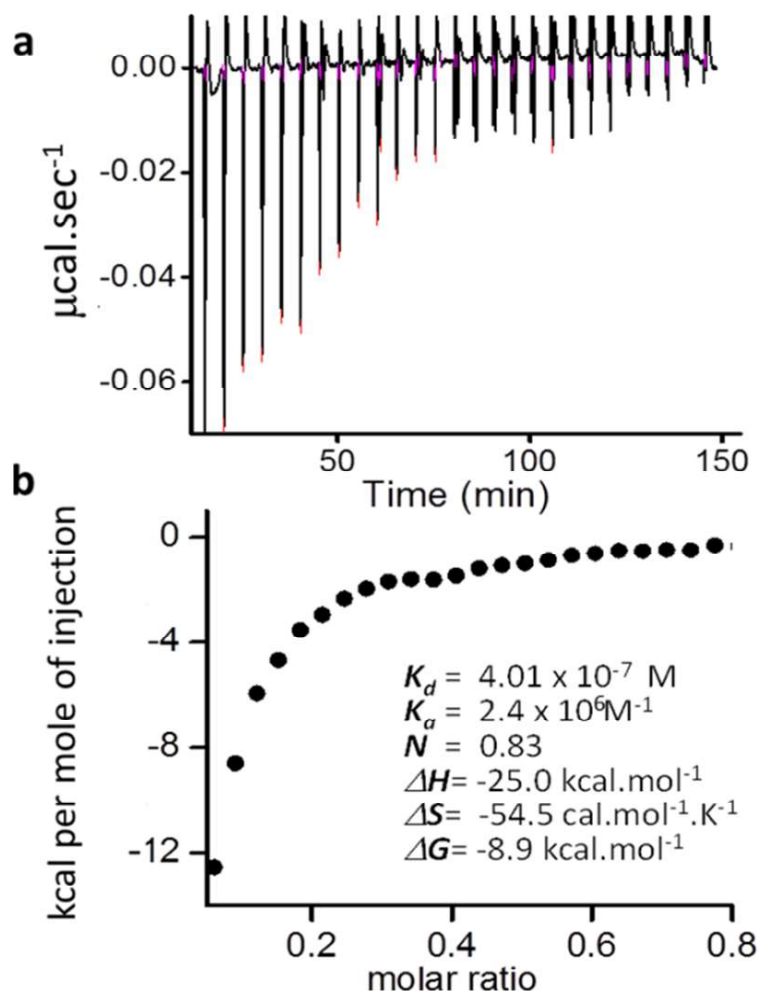
**Figure 6.13: Interaction of triple-helical collagen peptide with AuNPsHYP by Isothermal Titration Calorimetry (ITC).** (a) Base line subtracted raw data from ITC for titration of triple helical collagen model peptide (Pro-Hyp-Gly)10 (10 μ M) with ligand AuNPs$^{HYP}$(50 μM) at 298 K, showing the calorimetric response peaks in μcal.sec-1 during successive injections of AuNPs$^{HYP}$ to the peptide sample in the cell. (b) Integrated heat profile of data generated from ITC data. The solid line represents the minimized independent fitting by a model of one site per monomer (using Nano Analyze 2.1 software from Thermal Analysis). Inset of panel b displays the binding parameters obtained for AuNPs-peptide interaction.

Titration of Hyp-coated gold nanoparticles into a soluble sample containing (Pro-Hyp-Gly)$_{10}$ triple helical molecules showed affinity of AuNPs$^{HYP}$ for the triple helical structures. The obtained results, as shown in Figure 6.13, indicate affinity of Hyp for (Pro-Hyp-Gly)$_{10}$ triple helices, revealing important thermodynamic parameters of hydroxyproline-(Pro-Hyp-Gly)$_{10}$ interaction, as shown in the inset of Figure 4b ($Ka = 2.4 \times 10^6$ M$^{-1}$, $Kd = 4.01 \times 10^{-7}$ M, $\Delta H = -25.0$ kcal.mol$^{-1}$, $\Delta S = -54.5$ cal.mol$^{-1}$ K$^{-1}$, $\Delta G = -8.9$ kcal.mol$^{-1}$).

## 6.2 DISCUSSION.

This study has revealed that gold nanoparticles surface functionalized with hydroxyproline can effectively suppress the fibril formation of type I collagen under *in vitro* conditions. Since no suppression of collagen fibril formation was observed in the presence of free *Hyp* (uncoated), it appears that surface-functionalization of *Hyp* was critical for its available functional groups to interfere with the collagen-collagen interactions, causing the inhibition of fibril assembly. This assumption is supported by recent reports on the enhanced efficacies of the surface functionalized inhibitors due to gain of structural constraint (Anand et al., 2016; Porat, Abramowitz, & Gazit, 2006). The observation that Gly-coated nanoparticles did not suppress collagen fibril formation also suggests specific role of the functionalized-*Hyp* during suppression of collagen assembly.
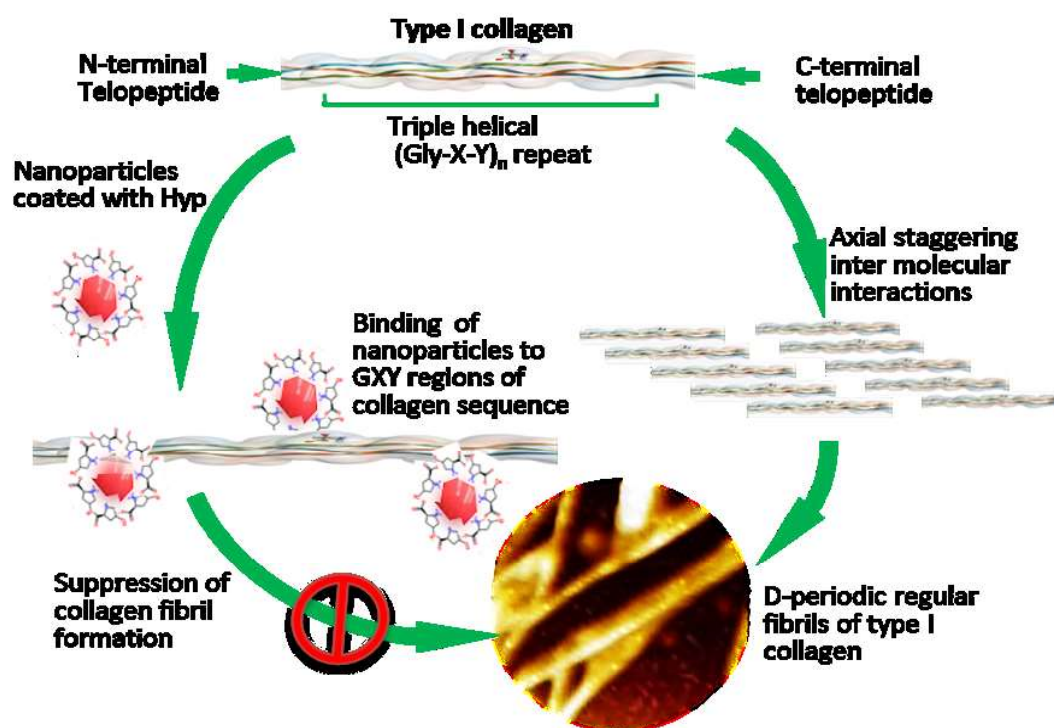


**Figure 6.14:** Schematic representation of targeting collagen fibril formation through gold nanoparticles surface-functionalized with hydroxyproline.

The binding data on the interaction between conjugated-*Hyp* with collagen model peptide (Pro-Hyp-Gly)$_{10}$ clearly suggest the affinity of *Hyp* residues for the triple helical (Gly-Pro-Hyp) domains. Such experimental data on contacts between AuNPs$^{HYP}$ and (Pro-Hyp-Gly)$_{10}$ was further supported by the computational docking studies where it clearly displayed the potential of the *Hyp* to interact with (Gly-Xaa-Yaa) triple helical conformers. Though it was difficult for us to conduct docking studies using conjugated-*Hyp* as a ligand due to limitations of docking protocols, it was assumed that the geometrical alternations, if any, due to the conjugation of -NH moiety of the *Hyp* molecule with the nanoparticles (after synthesis), would still allow its –COOH group and 4'–OH group to interact with the binding regions in the triple helical molecule. Docking studies on the triple helix of the collagen model peptide (PDB ID 1Q7D) shows hydroxyproline's affinity for the GFOGER sequence. More importantly, the Triple helical Telopeptide binding region (T-TBR) in the collagen molecule contains a –GFOGER–

stretch(Chung et al., 2008; Steplewski & Fertala, 2012). Hence, it appears that the binding of the AuNPs$^{HYP}$ with T-TBR may be one of the reasons behind the inhibition effect.

The question of which region of the collagen sequence is interacting with *Hyp* is very important because the longer sequence of type I collagen comprises imino acids, hydrophobic residues and charged residues, all of which are believed to be playing critical roles for driving fibril-assembly process. Considering ITC data on (Pro-Hyp-Gly)$_{10}$ peptide that displayed a single binding site for the ligand (surface-functionalized hydroxyproline), It was predicted that the possibility of multiple binding sites in type I collagen sequence to accommodate AuNPs$^{HYP}$ ligands (Figure 6.14). This assumption is further supported by the sequence analysis of type I collagen which displays regular occurrence of (Gly-Pro-Hyp) triplets spanning from C-terminal to N-terminal zone (Figure 6.9). Also, significant suppression effect on collagen fibril formation was observed only at 1:100 molar ratio of collagen: inhibitor whereas slight inhibition was observed at 1:25 molar ratio.

To explore the possibility of the effect of other amino acids on collagen fibril formation stable gold nanoparticles coated with *Pro* and *Trp* were synthesized. The characterization of these nanoparticles is shown in (Figure 6.3 and 6.4). *Pro* shares a similar structure like *Hyp*, without 4'–OH group and the presence of aromatic residues such as *Trp* and *Tyr* is already known to promote collagen-collagen contacts during fibril assembly (Kar et al., 2008). Interestingly, both of these nanoparticles, namely AuNPs$^{PRO}$ and AuNPs$^{TRP}$ showed similar inhibition effect on fibril formation of type I collagen (Figure 6.7, panel a). However, these amino acids (at similar concentration) in their free forms did not show any such inhibition effect (Figure 6.7), confirming the significance of their surface functionalization to show the inhibition effect. These results point to the ability of proline and aromatic molecules to interfere with the intermolecular aromatic-proline and aromatic-aromatic interactions necessary for collagen self-assembly. Generation of D-periodic fibrils of type I collagen is considered to be driven by both non-specific and specific interactions. Presence of *Hyp* may help in non-specific interactions (Leikin et al., 1995), whereas the interactions driven by hydrophobic(Kar et al., 2009a)(Cejas et al., 2008) and charged residues (Keshwani, Banerjee, Brodsky, & Makhatadze, 2013; Shyam Rele et al., 2007) are known to bring specific interactions between triple helical molecules. Hence, in addition to *Hyp* mediated driving forces, targeting intermolecular interactions mediated by charged residues and aromatic groups could also prove to be an effective strategy for inhibition of collagen fibril assembly. The physiochemical properties of the nanoparticles such as size and charge have been considered as critical factors for their antifibrotic properties. Here in this study, both the control gold nanoparticles (AuNPsGly) and the Hyp coated nanoparticles (AuNPsHyp) were found to be of similar size. Nanoparticles coated with Hyp, Pro and Tyr could suppress the collagen fibril formation where Gly coated nanoparticles did not show such inhibition effect. Though further experiments are certainly required to know how nanoparticle of different sizes can alter the fibril formation process of collagen, in the current study it was predicted that the functionalized amino acid is playing a dominant role during suppression of the collagen fibril formation.

*Hyp*-mediated osmolytic effect has been reported to influence both the conformational and aggregation properties of macromolecules, preferably through alterations in the solvation effect (Keswani, Kar, & Kishore, 2010)(Kar & Kishore, 2007). Sugar molecules have been reported to inhibit fibril formation of type I collagen, preferably through reordering of water molecules leading to solvent mediated inhibition effect(Kuznetsova & Leikin, 1999). However, such solvent mediated effect is observed only when these molecules are present at very high concentrations (in the range of 2M to 3M). In this study, the maximum concentration for hydroxyproline was maintained at ~100 μM. Hence, it is believed that the *Hyp*-induced solvation effects on collagen triple-helical molecules, if any, due to the presence of *Hyp* in the solution may not be sufficient to cause the prevention of collagen fibril formation. Again, only surface functionalized *Hyp,* not the free *Hyp*, is capable of suppressing the fibril formation,

suggesting direct interaction of AuNPs[HYP] with the collagen rather than the solvent mediated indirect interactions.

Though the pathophysiology of lethal collagen linked fibrotic growth in the body system is considered as a hetero-component assembly that includes different collagen types (type III, type V and type I), targeting fibril assembly of type I collagen is believed to be an effective strategy to reduce fibrosis complications (Chung et al., 2008)(Romanic, Adachi, Kadler, Hojima, & Prockop, 1991). Chung et al using a mouse model has already established the concept for reducing formation of fibrotic deposits by inhibiting self-assembly of collagen molecules into fibrils (Chung et al., 2008). Prevention of uncontrolled growth of collagen could benefit the treatment of severe pathologies including tissue fibrosis disorders and restenosis linked complications. For example curcumin coated stents have been reported to be effective in reducing restenosis complications and studies have also revealed that curcumin can influence collagen metabolism in model systems(Li et al., 2017; Wang et al., 2017). Targeted drug delivery devices such as the designing of magnetic nanoparticles coated with Hyp residues or making receptor specific microspheres loaded with Hyp coated gold nanoparticles can help in the prevention of the onset of these collagens activated diseases. Considering the vital role of *Hyp* mediated driving forces behind collagen self-assembly process, the results of this work establish the protective effect of AuNPs[HYP] against collagen fibril assembly. Crystal structures of collagen model peptides (Jordi Bella, Brodsky, & Berman, 1995; Barbara Brodsky & Persikov, 2005) have already revealed the *Hyp* mediated water bridges between triple helical molecules and it is believed that AuNPs[HYP] can effectively interfere with these fundamental forces. Though this work is an *in vitro* investigation, the results obtained could be beneficial to the researchers specifically targeting collagen activated diseases such as tissue fibrosis, in cell and animal models.

## 6.3 CONCLUSION.

The work done in this chapter reveals that gold nanoparticles coated with aromatic residues have the potential to prevent the fibril formation of type I collagen under *in vitro* conditions. This work has also successfully demonstrated the synthesis of the stable nanoparticles coated with the selected amino acids. These nanoparticles were found to be homogenous and of uniform size. Moreover, they were found to be hematocompatible.

...